Organometallic and Organic Dimers: Moderately Air-Stable, Yet Highly Reducing, n-Dopants

Swagat K. Mohapatra,[a] Seth R. Marder,[b,c,d]* and Stephen Barlow[b]*

a) Department of Industrial and Engineering Chemistry, Institute of Chemical Technology – Indian Oil Odisha Campus, IIT Kharagpur Extension Center, Bhubaneswar Odisha 751013, India; b) Renewable and Sustainable Energy Institute, University of Colorado Boulder, 4001 Discovery Drive, Boulder, CO 80303; c) Department of Chemical and Biochemical Engineering, University of Colorado Boulder, 3415 Colorado Avenue, Boulder, CO 80303; and d) Department of Chemistry, University of Colorado Boulder, 215 UCB, Boulder, CO 80309.

CONSPECTUS: Electrical doping using redox-active molecules can increase the conductivity of organic semiconductors and lower charge-carrier injection and extraction barriers; it has application in devices such as organic and perovskite light-emitting diodes, organic and perovskite photovoltaic cells, field-effect transistors, and thermoelectric devices. Simple one-electron reductants that can act as n-dopants for a wide range of useful semiconductors must necessarily have low ionization energies, and are thus highly sensitive towards ambient conditions, leading to challenges in their storage and handling. A

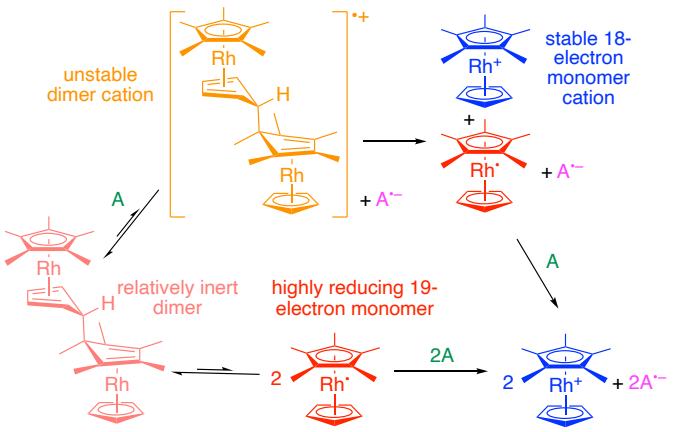

number of approaches to this challenge have been developed, in which the highly reducing species is generated from a precursor, or in which electron transfer is coupled in some way to a chemical reaction. Many of these approaches are relatively limited in applicability, due to processing constraints, limited dopant strength, and/or the formation of side products.

This account discusses our work to develop relatively stable, yet highly reducing, n-dopants based on the dimers formed by some 19-electron organometallic complexes and by some organic radicals. These dimers are sufficiently inert that they can be briefly handled as solids in air, but react with acceptors to release two electrons and to form two equivalents of stable monomeric cations, without formation of unwanted side products. We first discuss previously reported and our own syntheses of such dimers. We next turn to discuss their thermodynamic redox potentials, which depend on both the oxidation potential of the highly reducing odd-electron monomers and on the free energies of dissociation of the dimers; because trends in both these quantities depend on the monomer stability, they often more-or-less cancel, resulting in effective redox potentials for a number of the organometallic dimers that are ca. –2.0 V vs. ferrocenium/ferrocene. However, variations in the dimer oxidation potential and the dissociation energies determine the mechanism through which a dimer reacts with a given acceptor in solution: in all cases dimer-to-acceptor electron transfer is followed by dimer cation cleavage and a subsequent second electron transfer from the neutral monomer to the acceptor, but examples with weak central bonds can also react through endergonic cleavage of the neutral dimer, followed by electron-transfer reactions between the resulting monomers and the acceptor. We then discuss the use of these dimers to dope a wide range of semiconductors through both vacuum and solution processing. In particular, we highlight the role of photoactivation in extending the reach of one of these dopants, enabling successful doping of a low-electron-affinity electron-transport material in an organic light-emitting diode.

Finally, we suggest future directions for research using dimeric dopants.

KEY REFERENCES

- Guo, S.; Kim, S. B.; Mohapatra, S. K.; Qi, Y.; Sajoto, T.; Kahn, A.; Marder, S. R.; Barlow, S., N-Doping of Organic Electronic Materials Using Air-Stable Organometallics. *Adv. Mater.* **2012,** *24*, 699-703.[1] *This is our first report on the use of dimeric dopants, demonstrating the use of several organometallic sandwich dimers to increase conductivity in vacuum- and solution-processed organic semiconductors.*
- Mohapatra, S. K.; Fonari, A.; Risko, C.; Yesudas, K.; Moudgil, K.; Delcamp, J. H.; Timofeeva, T. V.; Brédas, J.-L.; Marder, S. R.; Barlow, S., Dimers of Nineteen-Electron Sandwich Compounds: Crystal and Electronic Structures, and Comparison of Reducing Strengths. *Chem. Eur. J.* **2014,** *20*, 15385–15394.[2] *This paper reports the crystal structures of six organometallic dimers, points out the lack of correlation between bond length and strength in these molecules, and compares effective dopant strengths (as quantified by Eq. 2 of the present Account).*
- Zhang, S.; Naab, B. D.; Jucov, E. V.; Parkin, S.; Evans, E. G. B.; Millhauser, G. L.; Timofeeva, T. V.; Risko, C.; Brédas, J.-L.; Bao, Z.; Barlow, S.; Marder, S. R., N-Dopants Based on Dimers of Benzimidazoline Radicals: Structures and Mechanism of Redox Reactions *Chem. Eur. J.* **2015,** *21*, 10878-10885.[3] *This paper reports the crystal structures of two organic dimers, and relates the electrochemistry and calculated bond strengths in three such dimers to their reactivity.*
- Lin, X.; Wegner, B.; Lee, K. M.; Fusella, M. A.; Zhang, F.; Moudgil, K.; Rand, B. P.; Barlow, S.; Marder, S. R.; Koch, N.; Kahn, A., Beating the Thermodynamic Limit with

Photo-Activation of n-Doping in Organic Semiconductors. *Nat. Mater.* **2017,** *16*, 1209-1215.[4] *This paper reports an application of an organometallic dimer to successfully dope a low-electron-affinity organic light-emitting diode material in a metastable fashion by using UV or visible photoactivation.*

INTRODUCTION

Electrical doping of organic semiconductors (OSCs) has emerged as a significant field of research, and has been applied in devices including organic light-emitting diodes (OLEDs), organic field-effect transistors (OFETs), and organic photovoltaic (OPV) cells, and, more recently, thermoelectric devices and lead-halide perovskite light-emitting diodes (PeLEDs) and solar cells (PSCs).[5-8] Generally electrical n- or p-doping is achieved by introducing chemical reductants or oxidants; typically the OSC consists of neutral closed-shell molecules or polymers, a fraction of which is converted to the corresponding radical anions or cations. Doping can greatly improve device performance by increasing conductivity – at low levels by filling charge-carrier traps due to impurities or structural defects and, at higher levels, by contributing mobile charge carriers (i.e., creating the aforementioned radical ions from which electrons or holes can hop to neighboring neutral moieties) – and by decreasing barriers to charge injection from electrodes.

Alkali metals were among the first n-dopants; however, their pyrophoric, highly reactive, and volatile nature complicates handling. Furthermore, small alkali cations readily diffuse within devices.[9] Larger molecular dopants can help minimize unwanted reactivity, restrict dopant-ion diffusion, and minimize electrostatic interactions between dopant ions and charge carriers, which will tend to trap the carrier on semiconductor molecules close to the dopant ions. The position of equilibrium for a solution electron-transfer reaction between a one-electron reductant and an electron-transport material (ETM) depends on the difference in redox potentials; ideally the reductant oxidation potential (E_{ox}) is significantly more negative than the ETM reduction potential (E_{red}). Similarly, efficient solid-state electron transfer requires a reductant solid-state ionization energy (IE) smaller than the ETM solid-state electron affinity (EA). Typical OPV and OLED ETMs exhibit $E_{red} \sim -1.0$ V and < -2.0 V vs. $FeCp_2^{+/0}$ (Cp = cyclopentadienyl), respectively

(roughly corresponding to EA ~ 3.8 and < 2.8 eV, although we emphasize there is no universal equation precisely relating solution E_{ox} / E_{red} and solid state IE / EA). Accordingly, even the weakest one-electron reductants suitable for OPV applications will be somewhat sensitive to atmospheric O_2 and H_2O, while stronger reductants for OLEDs will be considerably more so, complicating their storage and handling, e.g., decomposing during the brief air exposure often necessary when loading a solid sample into an evaporation crucible.

Several strategies to obtain more easily handled n-dopants involve coupling the electron transfer to additional chemistry. Some halide salts of stable conjugated organic cations (D^+X^-, e.g., PyB^+Cl^-, CV^+Cl^-, MeO-DMBI$^+$I$^-$, Figure 1)[10-13] liberate the corresponding reducing radicals, $D^\bullet$, on sublimation, presumably along with X_2.[12] However, their use is limited to vacuum-processing, and, at least in some cases, side products are obtained.[12] In certain circumstances, apparently redox-inert species such as simple amines[14] and tetraalkylammonium halides[15] can n-dope OSCs (Figure 1); these approaches are limited in applicability and afford side products.[16,17] More widely applicable are hydride-reduced derivatives of stable cations (DH, e.g., DH = LCV, Y-DMBI-H, Figure 1); these form D^+ cations on doping and are effective for fullerenes and some conjugated polymers,[11,18] although AH_x is formed as well as $A^{\bullet-}$ for A = fullerene,[11,19] and AH^- for A = 2CN-BDOPV.[20] For other ETMs, the side products are less clear, and doping cannot be predicted from ETM EA alone.[20]

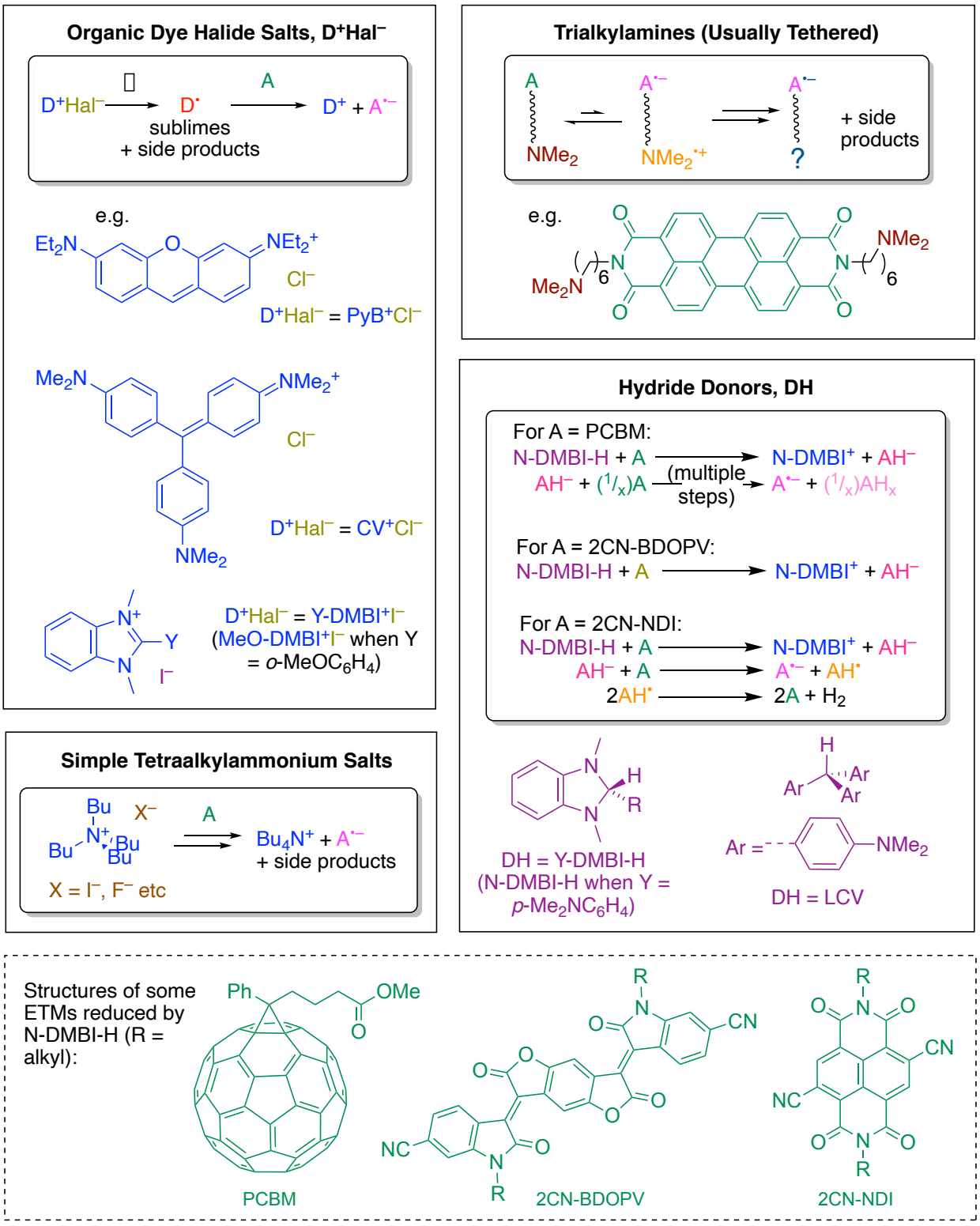

Figure 1. Some approaches for n-doping ETMs (A), in which bond breaking and/or formation is coupled to electron transfer.

We were interested in developing easily handled n-dopants that do not form side products and that can be processed both from solution and through evaporation. We recognized that some organic radicals ($D^{\bullet}$) could act as reductants, and that others formed relatively stable closed-shell dimers (D_2). We reasoned that if D_2 were sufficiently weakly bonded, it might act as a "masked" form of $D^{\bullet}$, liberating $D^{\bullet}$, e.g., by heating. The reversible dimerization of $Ph_3C^{\bullet}$ has been known for almost a century,[21] although $Ph_3C^{\bullet}$ is only weakly reducing (–0.11 V vs. $FeCp_2^{+/0}$).[22] The dimer obtained by reduction of nicotinimide adenine dinucleotide, $(NAD)_2$, has also long been known; $NAD^{\bullet}$ is more reducing than $Ph_3C^{\bullet}$,[23] and, at least in some cases, $(NAD)_2$ acts as a reductant in aqueous solution.[24] A $(NAD)_2$ analog, $(BNA)_2$, has been used as photoreductant for C_{60},[25] while related heteroarene dimers and $(Me\text{-}DMBI)_2$ have been used to reduce electrochemically-generated organic radicals (Figure 2).[26] We realized that some organometallic dimers might behave in a similar way and could be rather strong reductants. Here we describe our work to explore n-doping with dimers (D_2), both of 19-electron sandwich molecules and of organic radicals, that are moderately air stable and highly reducing, can be both solution and vacuum processed, and undergo clean reaction with semiconductors (A) to form only $A^{\bullet-}$ and the stable monomeric cation, D^+. We discuss the synthesis and structures of these dimers, their strength as reductants, their reactivity, and their use in n-doping of OSCs and other materials.

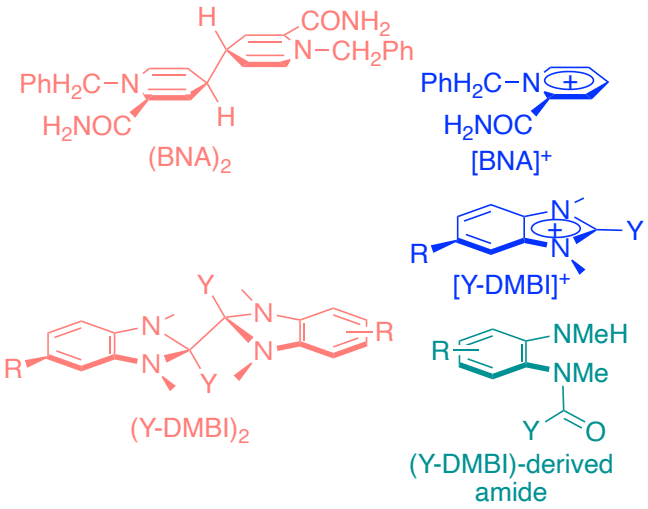

	Y	R
Me-DMBI	Me	H
Cyc-DMBI	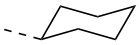	H
Fc-DMBI	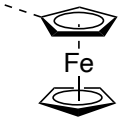	H
Rc-DMBI	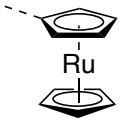	H
N-DMBI	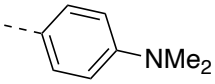	H
Cyc-DMBI-Me	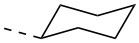	Me

Figure 2. Structures of dimeric organic reductants, corresponding cations, and amide side/decomposition product discussed in this Account.

2. SYNTHESIS AND STABILITY OF DIMERS

19-electron organometallic sandwich compounds are 1-electron reductants, readily forming the corresponding stable 18-electron cations. These include $CoCp_2$ (E_{ox} = –1.33 V vs. $FeCp_2^{+/0}$) and $CoCp^*_2$ (Cp* = C_5Me_5; –1.94 V), and some mixed-ring iron(I) species, such as $FeCp^*(C_6Me_6)$ (–2.30 V).[22] Indeed, our first ventures into n-doping OSCs were collaborations with Antoine Kahn's

group using $CoCp_2$ and $CoCp^*_2$, both of which are highly air and moisture sensitive and more volatile than ideal for vacuum processing using conventional crucibles.[27-29] However, stable 19-electron sandwich compounds of the 4d and 5d metals are almost unknown (an exception is the sterically congested 1,2,3,4,1',2',3',4'-octaphenylrhodocene[30,31]). If generated by reduction of the 18-electron D^+, most rapidly react to regain 18-electron configurations, in some cases by dimerization to D_2, and in others by forming DH, presumably via reaction with solvent, in either case undergoing a reduction by one unit of the hapticity of one of the rings.

In 1966 Fischer and Wawersik reported that $RhCp_2$ (Figure 3) existed as a dimer that was "moderately air stable" in the solid state.[32] Relevant to our doping strategy were their observations that $(RhCp_2)_2$ dissociated to $RhCp_2$ on sublimation, and that oxidation of $(RhCp_2)_2$ gave $RhCp_2^+$. Electrochemistry indicated the monomer was highly reducing (–1.85 V vs. $FeCp_2^{+/0}$) and shed additional light on the interconversion of $(RhCp_2)_2$ and $RhCp_2^+$.[33] Dimers were also reported for other rhodocenes,[34] iridocenes,[32,35] ruthenium(cyclopentadienyl)(arene) complexes,[36,37] and $M(C_6Me_6)_2$ (M = Tc, Re),[38,39] but these species were not widely studied as reductants. A few iron(cyclopentadienyl)(arene) derivatives also dimerize.[40-42]

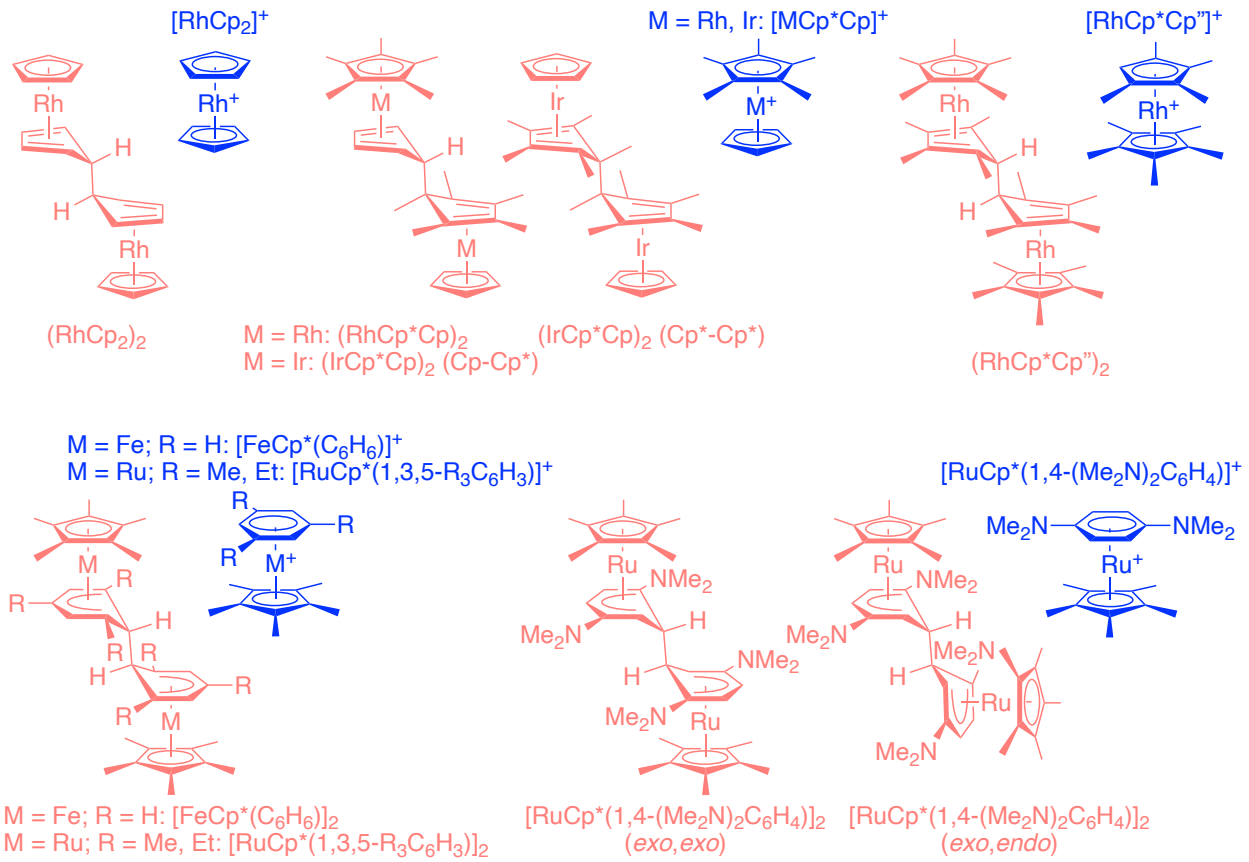

Figure 3. Structures of dimeric organometallic reductants and the corresponding monomeric cations studied by the authors.

Accordingly, we resynthesized $(RhCp_2)_2$ to examine as an n-dopant. To explore the generality of the approach, and to investigate the dimers of more strongly reducing monomers, we also synthesized other known dimers, D_2, with D = RhCp*Cp,[34] IrCp*Cp,[35] $FeCp^*(C_6H_6)$,[41] and $RuCp^*(1,3,5\text{-}Me_3C_6H_3)$,[36] (Figure 3) by reduction of $D^+PF_6^-$ in THF. We generally used 1 wt% Na:Hg or 1:3 (w/w) Na:K (CAUTION – pyrophoric liquid) as reductants,[1,43,44] although we have recently found that stage 1 silica-gel-supported Na:K (NaK_2-SG(I)), a commercially available solid stable to dry air,[45] is effective in some cases.[46,47] Electrochemical reduction of D^+ has also been used in the literature.[33-36]

New dimers we synthesized (Figure 3) include those for D = RuCp*(1,3,5-$Et_3C_6H_3$),[1] RhCp*Cp" (Cp" = C_5Me_4H),[2] and RuCp*(1,4-$(Me_2N)C_6H_4$).[47] However, 19-electron $D^{\bullet}$ formed on reduction of 18-electron sandwich D^+ do not necessarily dimerize: many 3d examples are stable (in the absence of air); many 4d and 5d D^+ form DH rather than D_2, apparently depending on an interplay of electronics and sterics (e.g., RuCp*(1,3,5-$Me_3C_6H_3$) dimerizes, but its C_6H_6 and C_6Me_6 analogues give DH[36]); and some undergo ligand redistribution (e.g., RuCp(C_6H_6) gives some $RuCp_2$[36]). We found: RuCp*(C_6Me_5H) and IrCp*Cp" fail to cleanly dimerize, giving intractable mixtures;[44,48] RuCp*(1,3,5-$^tBu_3C_6H_3$) forms products including the 18-electron deprotonation product Ru(η^4-$C_5Me_4CH_2$)(η^6-1,3,5-$^tBu_3C_6H_3$);[47] and RuCp*(1,3,5-$(Me_3SiCH_2)_3C_6H_3$) undergoes a second reduction to pyrophoric 18-electron K^+[RuCp*(η^4-1,3,5-$(Me_3SiCH_2)_3C_6H_3$)]$^-$.[44]

In the light of the reactivity we observed for organometallic dimers (section 4), we returned to consider organic dimers to fully explore the scope of the dimeric approach to n-dopants. 2-Substituted-2,3-dihydrobenzo[*d*]-imidazoles (Y-DMBI-H, Figure 1) were long known as reductants and first used as air-stable solution-processible n-dopants by Zhenan Bao's group.[18] They are effective for fullerenes and for some conjugated polymers, which accomodate the fairly planar [Y-DMBI]$^+$ without excessive loss of order.[49] We were interested in whether (Y-DMBI)$_2$ dimers could act as cleaner, more reactive sources of [Y-DMBI]$^+$ and $A^{\bullet-}$, without forming the hydrogen-reduced intermediates and/or side products expected from N-DMBI-H. (Me-DMBI)$_2$ (Figure 2) had been synthesized electrochemically from Me-DMBI$^+$ in the 1980s;[26] we used alkali-metal reductions of D^+ to obtain (Y-DMBI)$_2$ for Y = Cyc, Fc, Rc (collaboration with Bao),[50] and more recently (N-DMBI)$_2$.[46] Xioazhang Zhu's group obtained (Cyc-DMBI-Me)$_2$ in the same way.[51] A complication not encountered with the organometallic dimers is the formation of amide

side products (Figure 2), likely resulting from reaction of alkali hydroxides with D^+; careful control of reaction conditions and/or purification is needed to obtain clean D_2.

Crystal structures have been determined for examples of both classes of dimer and confirm the connectivity deduced from NMR (Figure 4).[2,3,47] For nearly every organometallic dimer the central C—C is on the opposite (*exo*) face of the ring through which dimerization takes place from the metal atom of each monomer. Recently, however, we isolated and crystallographically characterized an *exo,endo* isomer of $[RuCp^*(1,4\text{-}(Me_2N)C_6H_4)]_2$ (Figure 3, 4).[47] The central C—C portion of all the dimers is effectively either a tetra-, penta-, or hexa-substituted ethane and, as such, the C—C bonds are fairly long (1.54-1.64 Å; see section 3).

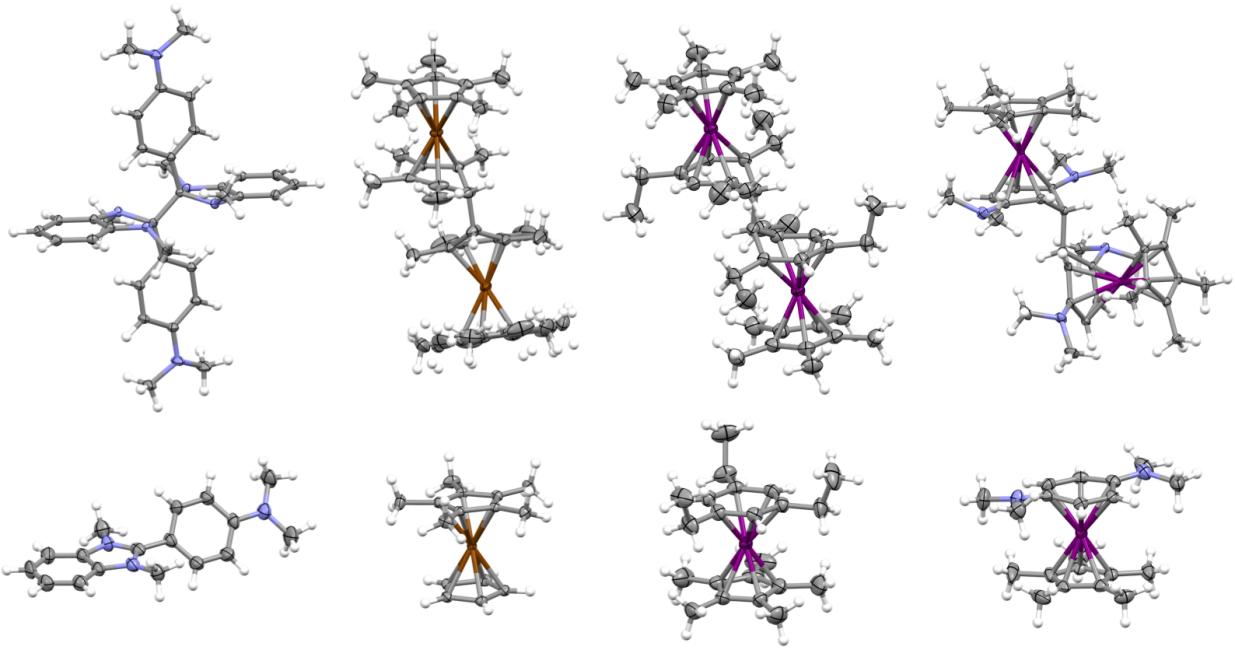

Figure 4. Crystallographically determined molecular structures for (above) representative dimers, D_2,[2,47,52] and (below) for the corresponding D^+ (PF_6^- salts).[44,46-48] From left to right: D = N-DMBI, RhCp*Cp, $RuCp^*(1,3,5\text{-}Et_3C_6H_3)$, and $RuCp^*(1,4\text{-}(Me_2N)C_6H_4)$ (*exo,endo* dimer isomer).

Both organometallic and DMBI dimers can be stored as solids in inert atmosphere for months without decomposition. Most – with $(RhCp^*Cp'')_2$ and *exo,exo*-$[RuCp^*(1,4\text{-}(Me_2N)C_6H_4)]_2$ notable exceptions (see below) – are sufficiently air stable that the solid can be briefly handled in ambient conditions, e.g., for weighing. However, they decompose slowly (rapidly in the case of the two noted exceptions) in solution on exposure to air: organometallic D_2 species give D^+, while $(Y\text{-}DMBI)_2$ convert quantitatively into the amides. In general, the organometallics are more stable in air than Y-DMBI dimers, likely due to the additional decomposition pathway possible for the latter class. Both the organometallic and Y-DMBI dimers are soluble in toluene, chlorobenzene, and THF, although $(RhCp_2)_2$ is rather poorly soluble; solutions in dry deoxygenated solvents are stable in inert atmosphere. Chloroalkanes, on the other hand, oxidize the dimers to D^+. It is worth noting that, despite the moderate air stability of the unreacted dopants, n-doped OSCs, except those with the highest EAs, are generally highly oxygen and water sensitive; accordingly, solution reactivity and doping studies (sections 4 and 5, respectively) have generally been carried out in inert atmosphere.

3. DOPANT STRENGTH

The thermodynamic strength of dimeric reductants, D_2, can be quantified by the effective redox potential for:

$$D^+ + e^- = 0.5D_2 \quad (1)$$

which is given by:

$$E(D^+/0.5D_2) = E(D^+/D) + \Delta G_{diss}(D_2) / 2F \quad (2)$$

where F is the Faraday constant. $E(D^+/D)$ is the potential for:

$$D^+ + e^- = D \quad (3)$$

and can be measured, or for less reversible cases estimated, from cyclic voltammetry of D^+. $\Delta G_{diss}(D_2)$ is the free energy of dissociation of the dimers:

$$D_2 = 2D \quad (4)$$

and is less easily determined. Y-DMBI• monomers are ESR-active organic radicals; in the case of $(Fc\text{-}DMBI)_2$ the bond is sufficiently weak that the solution concentration of D could be quantified by ESR and, together with the initial concentration of dimer, used to determine $[D]^2/[D_2]$ and, thus, $\Delta G_{diss}(D_2)$.[3] For the weakly bound $(RhCp^*Cp)_2$, we used:

$$\Delta G_{diss} = \Delta G^{\ddagger}_{diss} - \Delta G^{\ddagger}_{dim} \quad (5)$$

where $\Delta G^{\ddagger}_{diss}$ and $\Delta G^{\ddagger}_{dim}$ are the barriers for the dissociation of D_2 – inferred from reaction kinetics with an OSC, specifically from the temperature dependence of *k*' of eq. 7 (see section 4) and the dimerization of D – obtained from variable-temperature variable-scan-rate electrochemical measurements of the reduction / oxidation current ratio for D^+/D – respectively.[53] However, in general, we have relied upon DFT calculations of the energies of D_2 and D. In contrast to what is seen for weakly bound alkyl- and aryl-substituted ethanes,[54] DFT dissociation energetics are *not* correlated with either crystallographic or DFT central C—C bond lengths (Figure 5).[2,3] However, it is important to remember that bond length depends on orbital overlap and steric effects in D_2, whereas dissociation energy depends on *both* D_2 and D stability. Indeed, ΔU_{diss} for organometallic dimers increases with the expected trend in D instability (3d << 4d < 5d; higher < lower oxidation states). ΔU_{diss} trends for $(Y\text{-}DMBI)_2$ reflect more effective stabilization of the radical by metallocenyl or aryl substituents than by cyclohexyl.

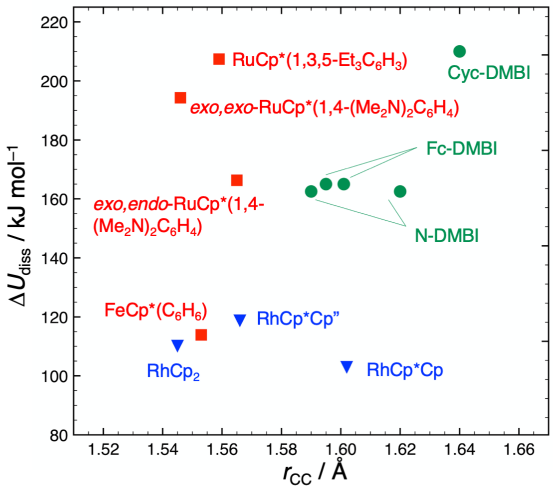

Figure 5. Plot showing no correlation between DFT-calculated dissociation energetics and crystallographic C—C bond lengths of D_2 (the structures of $(N\text{-DMBI})_2$ and $(Fc\text{-DMBI})_2$ contain two inequivalent molecules with different bond lengths). No correlation with DFT bond lengths is found either.

Figure 6 compares values of: $E(D^+/D)$; the potentials at which the dimers are irreversibly oxidized, $E(D_2^+/D_2)$; and of $E(D^+/0.5D_2)$ (estimated).[2,3] The range in $E(D^+/0.5D_2)$ is considerably smaller than that in $E(D^+/D)$; variations in the latter are often largely offset by those in ΔG_{diss}, both trends reflecting the stability of D. E.g., IrCp*Cp is both a more reducing monomer and more strongly dimerized than RhCp*Cp; the two effects reflect the greater tendency of the heavier metal to comply with the 18-electron rule and partially cancel to afford similar $E(D^+/0.5D_2)$. Similarly, Y = Cyc-DMBI has a stronger bond and a more reducing monomer than the other Y-DMBI derivatives. Variation in $E(D_2^+/D_2)$ is less readily rationalized; however, values for most indicate that electron transfer to O_2 would be endergonic ($E_{1/2}(O_2/O_2^{\bullet-}) = -1.2$ to -1.4 V), while the large $O_2/O_2^{\bullet-}$ reorganization energy and the moderate solubility of O_2 in aprotic solvents likely retard this initial step further, consistent with the moderate air stability of these compounds (see above).

Alkylation cathodically shifts $E(D^+/D)$ independently of dissociation energy, thus also shifting $E(D^+/0.5D_2)$, as seen in the rhodocene series; however, $E(D_2^+/D_2)$ is also cathodically shifted and that for $(RhCp^*Cp'')_2$ is comparable to $E(CoCp_2^{+/0})$, consistent with the air sensitivity of this dimer.

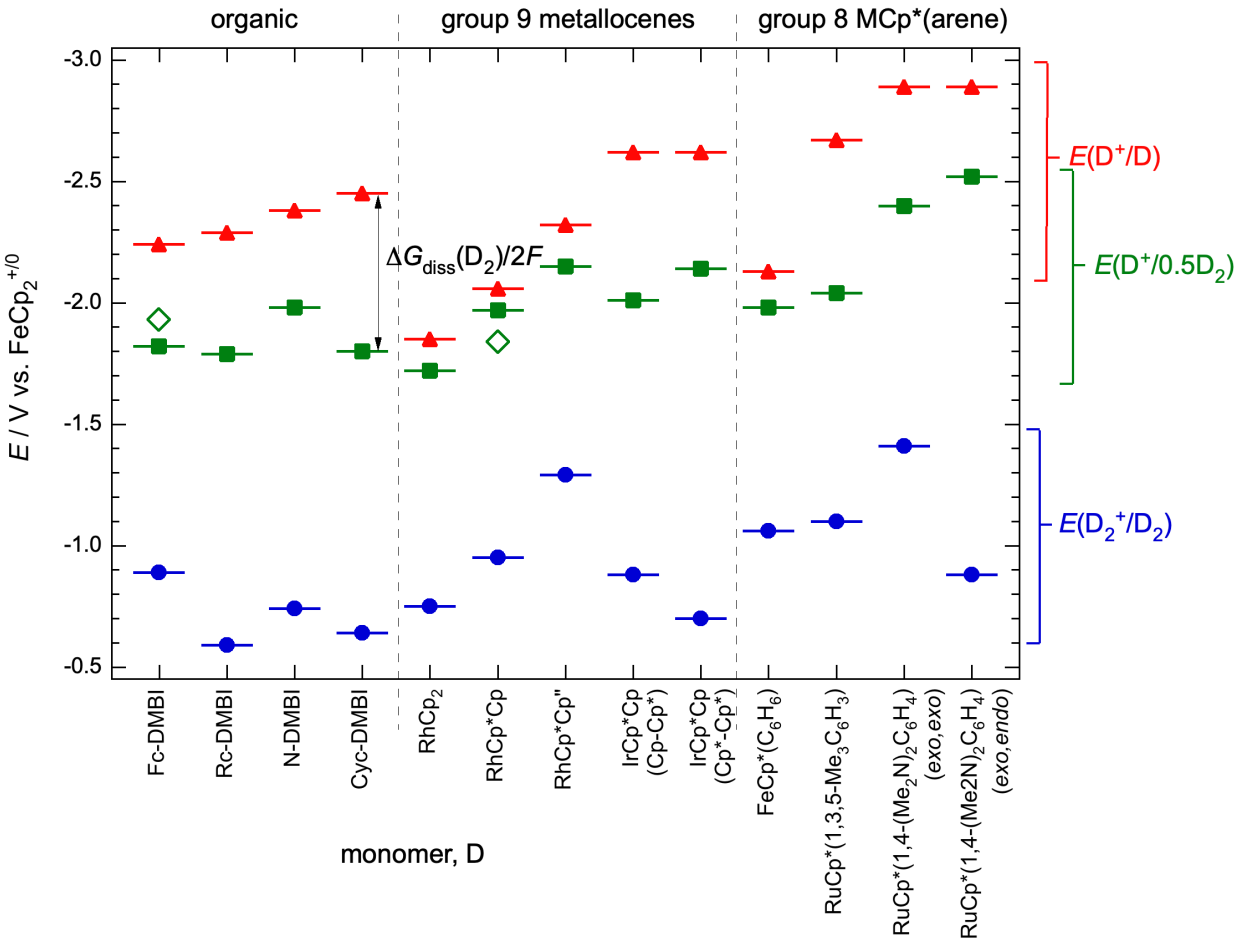

Figure 6. Electrochemical potentials relating to the reactivity of three types of dimeric reductants, each arranged in order of increasingly reducing monomers. $E(D^+/D)$ (red triangles) and $E(D_2^+/D_2)$ (blue circles) are from cyclic voltammetry; $E(D^+/0.5D_2)$ (green squares) is from eq. 2 using $E(D^+/D)$ and DFT-estimated $\Delta G_{diss}(D_2)$. Thus, (as indicated for one example) $E(D^+/D)$ – $E(D^+/0.5D_2)$ reflects ΔG_{diss}. Green diamonds represent $E(D^+/0.5D_2)$ estimated from experimental ΔG_{diss} values.

4. SOLUTION REACTIVITY

We initially envisaged that activation might be needed to "turn on" the doping reaction between dimers and OSCs. However, initial experiments on the solution reactivity of $(RhCp_2)_2$ and $[RuCp^*(1,3,5\text{-}Me_3C_6H_3)]_2$ with OSCs such as perylene diimides ($E_{red} \sim -1$ V) revealed rapid reaction, unsurprisingly in hindsight given the $E(D_2^+/D_2)$ potentials (Figure 6). Less easily reduced A = TIPS-pentacene ($E^{0/-} = -1.45$, $E^{-/2-} = -1.93$ V, Figure 7) gave more useful insight into D_2 reactivity. Its bulky substituents often impart solubility to $D^+A^{\bullet-}$, and in some cases $(D^+)_2A^{2-}$, even in solvents such as d_6-benzene (allowing D^+ to be identified by NMR) and chlorobenzene; the vis-NIR spectra of A, $A^{\bullet-}$, and A^{2-} are easily distinguishable (Figure 8); and the reactions timescales are often suitable for be monitoring by vis.-NIR spectroscopy. We have also obtained crystal structures of two D^+[TIPS-pentacene]$^{\bullet-}$ products.[43]

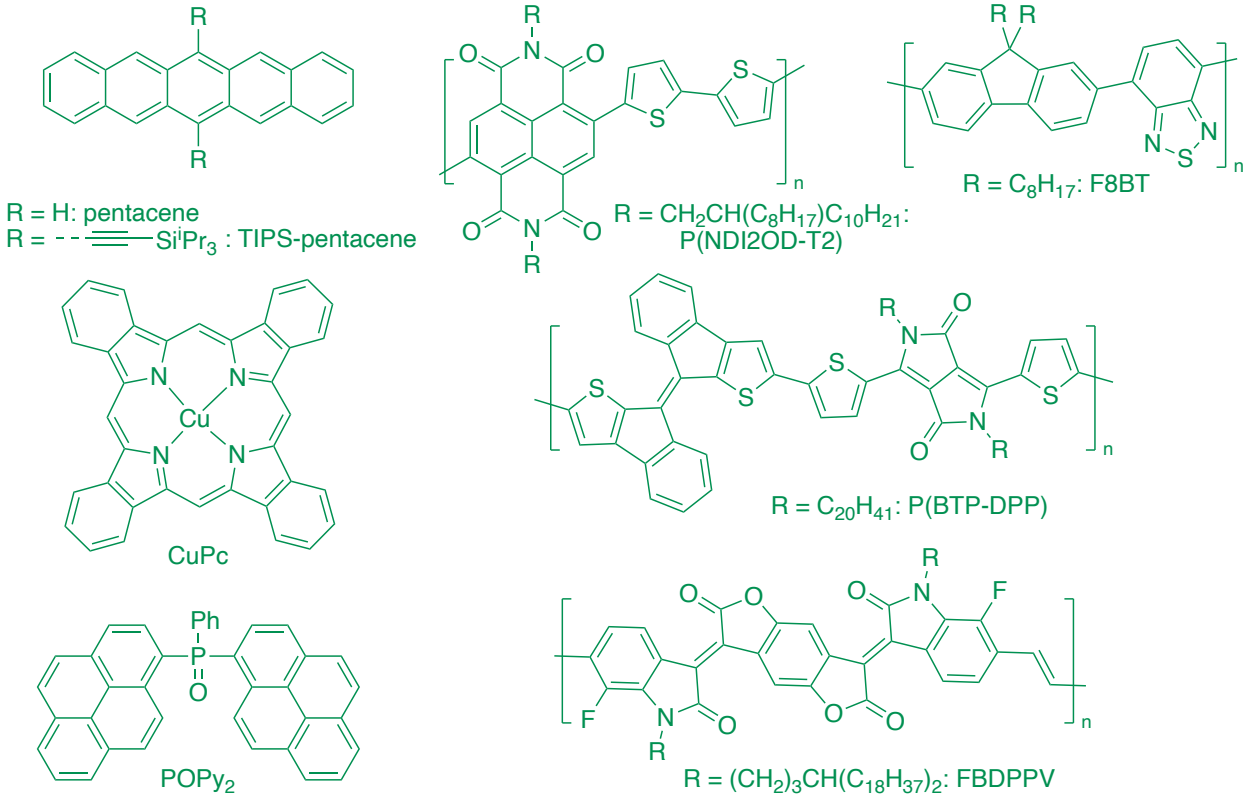

Figure 7. Structures of small molecules and polymers discussed in the context of reduction by D_2 n-dopants.

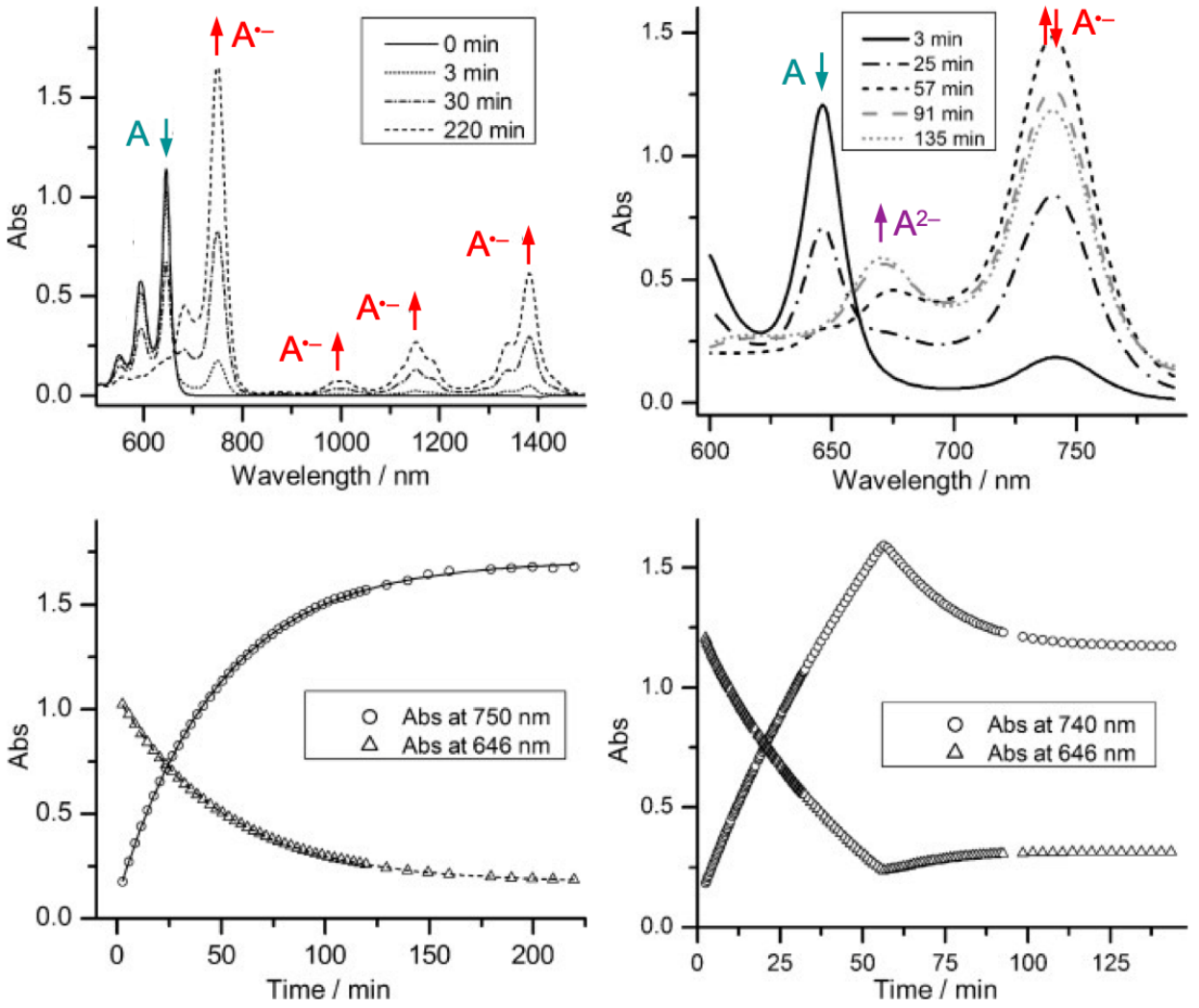

Figure 8. Top: Vis.-near-IR absorption spectra showing the reaction in chlorobenzene of TIPS-pentacene (A) with (left) excess $[RuCp^*(1,3,5\text{-}Et_3C_6H_3)]_2$ and (right) excess $(RhCp^*Rh)_2$. Bottom: corresponding temporal evolutions of absorbances at maxima characteristic of A and $A^{\bullet-}$ from the spectra (solid fits in the left plot indicate a reaction first order in TIPS-pentacene). Adapted from Ref. 43 with permission; copyright 2012 Wiley-VCH Verlag GmbH & Co. KGaA, Weinheim.

In contrast to the relatively limited range of $E(0.5D_2/D^+)$ (section 3), D_2 reactivity is more diverse. $[RuCp^*(1,3,5\text{-}R_3C_6H_3)]_2$ (R = Me, Et) and TIPS-pentacene react according to:

$$^1/_2[A^{\bullet-}]/dt = d[D_2]/dt = k[D_2][A] \quad (6)$$

and the barrier, $\Delta G^{\ddagger}$ (obtained from the temperature-dependence of k) is consistent with electrochemical estimates of ΔG for D_2-to-A electron transfer.[43] Only [TIPS-pentacene]$^{\bullet-}$ is formed, even when D_2 is in excess (Figure 8). This is consistent with a rate-determining initial D_2-to-A electron-transfer ("ET first", similar to previously proposed for the reaction of $(Me\text{-}DMBI)_2$ with [diphenylanthracene]$^{\bullet+}$[26]). For $(RhCp^*Cp)_2$:

$$^1/_2[A^{\bullet-}]/dt = d[D_2]/dt = k[D_2][A] + k'[D_2] \quad (7)$$

and A^{2-} is formed by excess D_2 (Figure 8), suggesting that the mechanism seen for the Ru compound occurs *in parallel* to another pathway with an initial rate-determining D_2 dissociation ("cleavage first"). This tendency of rhodocene dimers to cleave is consistent with NMR experiments that indicate that sublimation of a $[Rh(C_5(CD_3)_5)Cp]_2$ and $[RhCp^*(C_5D_5)]_2$ mixture affords a mixture of the two homodimers and the $Rh(C_5(CD_3)_5)Cp/RhCp^*(C_5D_5)$ heterodimers (similar experiments in solution are complicated by other H/D scrambling processes),[43] and with previous observations that $RhCp_2$ monomer can be trapped when subliming $(RhCp_2)_2$.[32] On the other hand, crossover is not observed when mixing $[RuCp^*(1,3,5\text{-}Me_3C_6H_3)]_2$ and $[RuCp^*(1,3,5\text{-}Et_3C_6H_3)]_2$ in solution, or on co-sublimation of $[RuCp^*(1,3,5\text{-}(CD_3)_3C_6H_3)]_2$ and $[RuCp^*(1,3,5\text{-}Me_3C_6D_3)]_2$, consistent with higher DFT ΔU_{diss} for the Ru dimers than for the Rh species (cf. separation of $E(D^+/0.5D_2)$ and $E(D^+/D)$ values in Figure 6). Figure 9 compares energetics for the reaction of these two dimers with TIPS-pentacene, obtained from a mixture of DFT and electrochemical data, emphasizing the similar overall ΔG, but differing intermediate energies and, therefore, different feasible pathways. Other strongly bonded dimers – $(Cyc\text{-}DMBI)_2$ and $(IrCp^*Cp)_2$ – barely react with TIPS-pentacene at room temperature,[2,3] although for the former we observed the ET-first reaction at higher temperatures. In both cases the reaction is accelerated by

visible light (presumably by electron transfer from D_2 to photoexcited A), thus approaching our original concept of activating doping by an external stimulus.[2,3] Weakly bonded $(Rc\text{-}DMBI)_2$ behaves similarly to $(RhCp^*Cp)_2$, while $(Fc\text{-}DMBI)_2$ reacts through a "cleavage first" pathway, but apparently with the second step rate-determining.[3] Cleavage also plays roles for *exo,endo*-$[RuCp^*(1,4\text{-}(Me_2N)C_6H_4)]_2$ and $(N\text{-}DMBI)_2$.[47,52] Despite DFT indicating a weak bond, $[FeCp^*(C_6H_6)]_2$ reacts with TIPS-pentacene via ET-first;[43] this and the slow dimerization of $FeCp^*(C_6H_6)$ were attributed to a particularly high-energy transition state for this D_2 / D interconversion, perhaps resulting from the greater localization of spin density on the metal, and its reduced extension onto the ligand, for $FeCp^*(C_6H_6)$ than for the 4d and 5d monomers.[53] Finally, $(RhCp^*Cp'')_2$ and *exo,exo*-$[RuCp^*(1,4\text{-}(Me_2N)C_6H_4)]_2$ react much more rapidly than any of the other dimers,[2,47] consistent with their especially cathodic $E(D_2^+/D_2)$ values. From a practical doping point of view, dimers that undergo cleavage are expected to achieve their thermodynamic doping limits relatively easily, while for strong bound dimers, D_2:A combinations that do not react in solution in the dark may permit processing in air with photoactivation of doping being carried out subsequent to encapsulation.

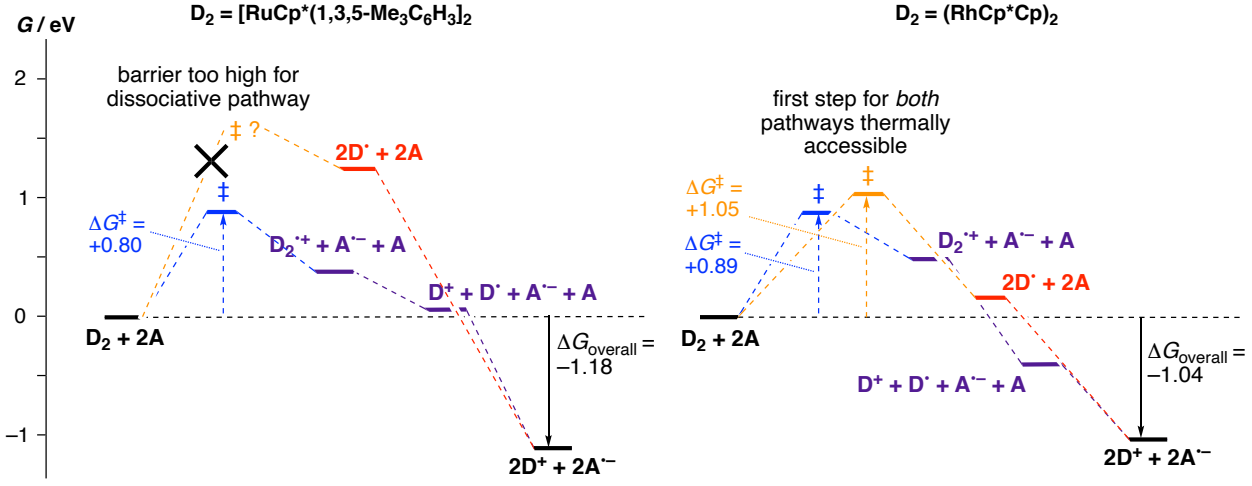

Figure 9. Free energies estimated using electrochemical and DFT data for the solution reactions of two dimers with TIPS-pentacene, along with experimental barriers for the rate-determining first steps. Note that although the overall energetics and those for the first step of the "ET-first" pathway (blue) are similar for the two dimers, those for the "cleavage first" pathway (red) are very different.

5. DOPING BEHAVIOR

In our first study of the organometallic dimers, Antoine Kahn's group demonstrated that coevaporation of $(RhCp_2)_2$, $[RuCp^*(1,3,5\text{-}Me_3C_6H_3)]_2$, or $[FeCp^*(C_6H_6)]_2$ with CuPc (Figure 7, EA = 3.1 eV) resulted in effective n-doping, indicated by a shift of the Fermi level to within 0.15–0.37 eV of the onset of empty OSC states, and, for the Fe and Rh dopants, a six-orders-of-magnitude enhancement of current density.[1] All are much less air sensitive than $CoCp^*_2$ – one of the few reductants previously shown to n-dope CuPc – and have reduced volatility, compatible with standard crucible evaporation. $[RuCp^*(1,3,5\text{-}Me_3C_6H_3)]_2$ was also shown to be an effective vacuum-processible n-dopant for TIPS-pentacene (Figure 7, EA = 3.0 eV according to inverse photoelectron spectroscopy (IPES), lower than estimated from $E(A^{0/\bullet-})$ using standard approaches, underlining the unreliability of such estimates) and unsubstituted pentacene (Figure 7, EA = 2.8 eV). n-Doped films were also obtained by spin-coating solutions of $[RuCp^*(1,3,5\text{-}Me_3C_6H_3)]_2$ or $(RhCp_2)_2$ with TIPS-pentacene. Naturally a wide range of less challenging (higher EA) materials, such as those relevant to OPV and PSCs, can also be n-doped with dimers. In addition to co-sublimation and spin-coating from mixed solutions, sequential deposition has also been used (see second $[RuCp^*(1,3,5\text{-}Me_3C_6H_3)]_2$:P(NDI2OD-T2) entry and the $[RuCp^*(1,3,5\text{-}Me_3C_6H_3)]_2$:P(BTP-DPP) entry in Table 1);[55] however, its effectiveness depends on the dopant:host combination and the doping conditions.[55,56]

Table 1. Some Electrical Conductivities (σ) Obtained in OSCs Using Dimeric n-Dopants.

OSC, A (EA / eV)[a]	D_2	D_2:A[b]	Processing[c]	σ[d] / S cm^{-1}	Ref.
C_{60} (3.9)	$(Fc\text{-}DMBI)_2$	0.25	Coevaporation	8.0×10^{-2}	50
	$(Rc\text{-}DMBI)_2$	0.22	Coevaporation	1.0×10^{-1}	50
	$(Cyc\text{-}DMBI)_2$	0.35	Coevaporation	12	50
	$[RuCp^*(1,3,5\text{-}MeC_6H_3)]_2$	0.12	Coevaporation	8.3	57
$PC_{61}BM$ (3.8[e])	$(Fc\text{-}DMBI)_2$	0.06	Spin coating of D_2 and A from PhCl	1.9×10^{-3}	50
	$(Rc\text{-}DMBI)_2$	0.12	Spin coating of D_2 and A from PhCl	1.6×10^{-2}	50
	$(Cyc\text{-}DMBI)_2$	0.11	Spin coating of D_2 and A from PhCl	4.7×10^{-2}	50
$POPy_2$ (2.2)	$[RuCp^*(1,3,5\text{-}MeC_6H_3)]_2$	0.10	Coevaporation	5×10^{-10}	4
	$[RuCp^*(1,3,5\text{-}MeC_6H_3)]_2$	0.10	Coevaporation, UV activation	1×10^{-4}	4
FBDPPV (4.3[f])	$(N\text{-}DMBI)_2$	0.12	Spin coating of D_2 and A from toluene	8	46
	$[RuCp^*(1,3,5\text{-}MeC_6H_3)]_2$	0.30	Spin coating of D_2 and A from toluene	1.6	46
P(NDI2OD-T2) (3.9)	$(Fc\text{-}DMBI)_2$	0.35	Spin coating of D_2 and A from *o*-$Cl_2C_6H_4$	7.6×10^{-5}	50
	$(Rc\text{-}DMBI)_2$	0.14	Spin coating of D_2 and A from *o*-$Cl_2C_6H_4$	3.0×10^{-3}	50

	(Cyc-DMBI)$_2$	0.12	Spin coating of D_2 and A from *o*-$Cl_2C_6H_4$	2.8×10^{-3}	50
	(RhCp*Cp)$_2$	0.004	Spin coating of D_2 and A from toluene	9.5×10^{-5}	58
	[RuCp*(1,3,5-MeC_6H_3)]$_2$	0.06	Spin coating of D_2 and A from toluene	4.2×10^{-3}	59
	[RuCp*(1,3,5-MeC_6H_3)]$_2$	–	Immersion of A film in BuOAc solution of D_2 at 80 °C (5 min air exposure)	1.2×10^{-5}	56
P(BTP-DPP) (3.8[g])	[RuCp*(1,3,5-MeC_6H_3)]$_2$	0.27	Casting from toluene onto polymer film, 80 °C annealing	4.5×10^{-1}	55
F8BT (2.8)	[RuCp*(1,3,5-MeC_6H_3)]$_2$	0.24	Spin coating D_2 and A from toluene/PhCl	10^{-9}	60
	[RuCp*(1,3,5-MeC_6H_3)]$_2$	0.24	Spin coating of mixture, UV irradiation	10^{-6}	60

[a]From IPES unless otherwise stated. [b]Ratio of D_2 molecules to A molecules or polymer repeat units (ratio electrons to A will be tiwce this assuming complete D_2/A reaction). [c]In inert atmosphere unless otherwise noted. [d]Measurement methods vary between studies, so detailed comparisons should be made with care. [e]From ref. [61]. [f]Estimated from electrochemistry in ref. [49]. [g]From UPS IE, optical measurements, and estimated exciton binding energy.

Although n-doping of OSCs with EA ~ 3 eV is impressive, there is relatively little *technological* demand for n-doping materials in this particular range; OLED ETMs have even lower EAs, while those of typical OPV, OFET, and thermoelectric materials are much larger. Nonetheless, these dimers may still have some advantages for doping high-EA semiconductors in terms of stability, the variety of dopant ion sizes and shapes accessible (see below), and their easy vacuum or solution processibility. In addition, the large driving forces for doping in these systems are expected to lead to complete reaction to form D^+ and $A^{\bullet-}$, which is a necessary, but not sufficient, requirement for obtaining high doping efficiency (defined as the number of free charge carriers contributed per dopant molecule). Although doping efficiency has not yet been studied using D_2 doping, complete reactions are seen in solution for dimers with fullerenes, rylene diimides, and even lower-EA TIPS-pentacene.[3,20,43,47] Furthermore, X-ray photoelectron spectroscopy on $[RuCp^*(1,3,5\text{-}Me_3C_6H_3)]_2$-doped and P(BTP-DPP) and FBDPPV films show the Ru $3d_{5/2}$ ionization at binding energies consistent with $[RuCp^*(1,3,5\text{-}Me_3C_6H_3)]^+$, with no signal detectable at that of $[RuCp^*(1,3,5\text{-}Me_3C_6H_3)]_2$, indicating essentially complete reaction.[46,55]

Furthermore, the large driving forces, coupled with the multi-step nature of the doping reaction, ensure doping of high-EA OSCs is effectively irreversible. In contrast doping with weaker simple one-electron reductants may be reversible, leading to dedoping: P(NDI2OD-T2) n-doped with $[RuCp^*(1,3,5\text{-}Me_3C_6H_3)]_2$ is more resistant to air than when n-doped with $CoCp_2$ where rapid aerial oxidation of the equilibrium fraction of neutral $CoCp_2$ is thought to occur.[56] Sublimation of neutral fractions of weak dopants is also a possibility; this has been invoked to explain the rapid dedoping of poly(3-hexythiophene) p-doped with 2,3,5,6-tetrafluoro-7,7,8,8-tetracyanoquinodimethane.[62]

In collaboration with Koch, Kahn, and Rand groups we have found one of the organometallic dimers, $[RuCp^*(1,3,5\text{-}Me_3C_6H_3)]_2$, *can* n-dope several OLED ETMs (Figure 7, Table 1) – small molecules, particularly $POPy_2$,[4] and the polymer F8BT[60] – when photo-irradiated. Doping of $POPy_2$ is remarkable; at least based on $E(A/A^{\bullet-})$ (–2.24 V), it is beyond the estimated thermodynamic doping reach of the dimer (–2.04 V) (Figure 10), with doping likely of marginal energetic feasibility at best in the solid state, yet its conductivity is greatly enhanced by UV, or, to a lesser extent, visible irradiation, the enhancement being largely retained on removal of the light source (Table 1). The doping seems to occur through electron transfer from D_2 to UV-excited $POPy_2$ or through visible excitation of a D_2:$POPy_2$ charge-transfer (CT) complex. The stability of the doping, despite the overall estimated thermodynamics, is attributed to the activation barriers for the endergonic steps required for dedoping, and perhaps also with bringing monomeric cations, which may have diffused apart or reoriented subsequent to doping, back into the correct relative position to redimerize.

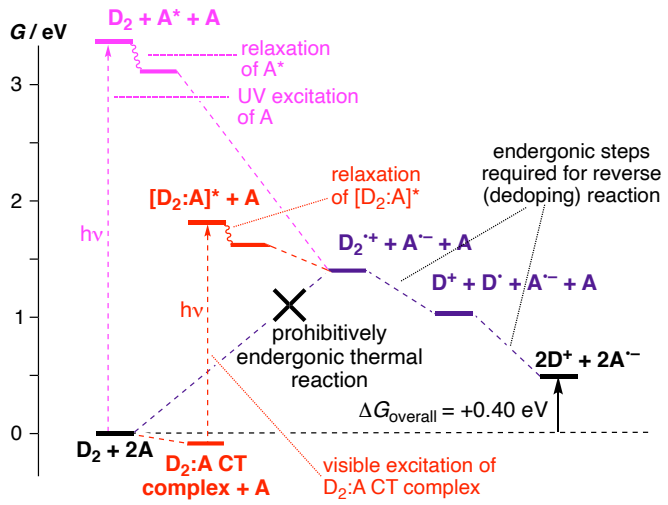

Figure 10. Free-energies estimated using electrochemistry and DFT for the reaction of $[RuCp^*(1,3,5\text{-}Me_3C_6H_3)]_2$ with $POPy_2$ showing UV (magenta) or visible (red) photoactivation pathways.

For sequential doping, some diffusion of dopant molecules and/or ions into the OSC is necessary for effective doping, but where spatially confined doping is desired, diffusion is disadvantageous. The relatively bulky organometallic sandwich cations have allowed thermally stable spatially confined doping to be achieved using the corresponding dimers in several semiconductors.[1,4] On the other hand, bulky dopant ions can disrupt more the packing of the OSC, potentially adversely affecting charge-carrier transport, as shown in a collaboration with the Pei and Yee groups:[46] FBDPPV (Figure 7) doped with $[RuCp^*(1,3,5\text{-}Me_3C_6H_3)]_2$ retains much less crystallinity of the pristine polymer and has lower conductivity than when doped with either N-DMBI-H or $(N\text{-}DMBI)_2$, which both form the more planar N-DMBI$^+$ cation. $(N\text{-}DMBI)_2$ and N-DMBI-H afford similar maximum conductivities, but at loadings of 43 and 11 mol% respectively, which attributed to cleaner and/or more complete reaction with the dimer (note $(N\text{-}DMBI)_2$ potentially contributes twice the electrons of N-DMBI-H and so, if both were 100% efficient, these doping levels should differ by only a factor of two). Different cation shapes may also be partly responsible for the large differences in conductivity of C_{60} doped by coevaporation by different $(Y\text{-}DMBI)_2$ species (Table 1).[50]

Although much of the preceding discussion focuses on electrical conductivities, it is important to realize that this is not the only OSC characteristic that can be enhanced by doping. E.g., high levels of bulk doping in OFETs severely compromises on/off ratios, but ultralow doping can decrease threshold voltage by filling traps, as demonstrated with $[RuCp^*(1,3,5\text{-}Me_3C_6H_3)]:C_{60}$,[63] while heavier doping levels at the source/drain contacts can increase the effective mobility through reducing contact resistance, as demonstrated with $(RhCp)_2:C_{60}$.[64]

In addition to the doping of OSCs, the dimers have also been used: to decrease the work function and increase the conductivity of two-dimensional materials such as graphene,[65,66] black phosphorus,[67] and few-layer group 6 metal dichalcogenides;[68,69] to convert ambipolar single-walled carbon nanotube transistors to n-channel devices;[66] and to decrease the work function of inorganic (semi)conductor surfaces.[70-72] A particularly low work function of 2.2 eV was obtained for a ZnO crystal, allowing its band positions to be aligned with the frontier orbitals of a planarized quaterphenyl derivative, converting a "type II" heterojunction, at which emission is quenched by exciton dissociation, to a highly emissive "type I" junction.[70]

Besides the above-mentioned organic and nanotube transistors, dimers have shown promising performance in other functional devices. $[RuCp^*(1,3,5\text{-}Me_3C_6H_3)]_2$:$POPy_2$ was shown to be an effective electron-injection layer for OLEDs, either when photoactivated externally, or "self-activated" through the initially inefficient OLED photoactivating doping, leading to improved electron injection and increased efficiency. Use of photoactivated $[RuCp^*(1,3,5\text{-}Me_3C_6H_3)]_2$:$POPy_2$ as an electron-injection layer, together with other innovations, has facilitated some of the most stable and efficient PeLEDs to date.[73] $(RhCp^*Cp)_2$-modification of fluorine-doped tin-oxide improves its effectiveness as an electron-collecting electrode in contact with organic ETMs in PSCs.[74] Nevertheless, further work is needed to understand the performance and stability of a wider variety of devices based on different D_2:A combinations; e.g., the diffusional stability of dopant ions mentioned above has only been studied for a handful of systems.

5. SUMMARY AND OUTLOOK

The organometallic and organic dimers discussed in this Account exhibit an unusual combination of characteristics, which has led to their use as n-dopants in a wide range of studies.

They are strongly reducing in a thermodynamic sense and so are powerful n-dopants, yet many are relatively kinetically inert, allowing their handling in air. In some cases, doping can be activated subsequent to processing of D_2:OSC films. Furthermore, for some [RuCp*(1,3,5-$Me_3C_6H_3$)]$_2$:OSC combinations, marginally stable or metastable doping has also been achieved.

Can even stronger reductants can be developed based on this approach? A challenge in that more reducing monomers can sometimes form more strongly bonded dimers, with little overall change in $E(D^+/0.5D_2)$,[2] although such species may be useful for activated and metastable doping. In other cases, more sensitive dimers are obtained.[2] However, our recent unexpected finding that *exo*,*endo* dimers can be formed in some cases suggests another means of combining very reducing $E(D^+/0.5D_2)$ and moderate stability,[47] although we do not yet know how to rationally obtain such isomers. We also see little practical need, at least in the context of organic electronics, for doping materials with substantially lower EA than $POPy_2$, which can be doped using existing dimers, albeit in a likely metastable manner.[4]

On the other hand, it may be useful to activate n-doping (either thermodynamically stable or metastable) of relatively high-EA materials, such as those used for thermoelectric, transistor, or photovoltaic applications, *subsequent* to solution film processing, e.g., to avoid precipitation of doped material, or to facilitate deposition in air and activation subsequent to encapsulation. This clearly requires D_2 that are weaker *and* that have relatively strong bonds (to avoid reaction by the "cleavage-first" pathway). While some dopants of other classes, such as DMBI-H derivatives, fulfil these requirements for some OSCs, their reactivity varies significantly with OSC.[20] Depending on their dissociation energetics, derivatives of the known $(BNA)_2$[25] may be promising.

If doping of $POPy_2$ with $[RuCp^*(1,3,5\text{-}Me_3C_6H_3)]_2$[4] is indeed metastable, it may be possible to reverse photoactivated doping in these or other systems, either thermally or optically, leading to externally "switchable" doping. Given the success of the dimeric approach to n-dopants, can an analogous approach afford water-inert but highly oxidizing p-dopants? While the molecular halogens represent a proof-of-principle, larger examples would be desirable for reduced volatility and accessing a wider range of dimer stabilities, dopant strengths, and reactivities. Finally, dimers exhibiting additional functionality may be interesting; e.g., covalent attachment of dopant ions to OSCs – demonstrated for DMBI-H-type n-dopants,[75] but not for dimers – can help preclude dopant-ion drift and diffusion and associated device instabilities.

AUTHOR INFORMATION

Corresponding Authors

Seth R. Marder - Renewable and Sustainable Energy Institute, Department of Chemical and Biochemical Engineering, and Department of Chemistry, University of Colorado Boulder, Boulder, CO 80303, United States; Email: seth.marder@colorado.edu

Stephen Barlow – Renewable and Sustainable Energy Institute, University of Colorado Boulder, Boulder, CO 80303, United States; Email: stephen.barlow@colorado.edu

Author

Swagat K. Mohapatra – Department of Industrial and Engineering Chemistry, Institute of Chemical Technology – Indian Oil Odisha Campus, IIT Kharagpur Extension Center, Bhubaneswar Odisha 751013, India

Notes

The authors declare no competing financial interest.

Biographies

Swagat K. Mohapatra received his M.Sc. from NIT Rourkela, India and Ph.D. in Chemistry from University of Pisa, Italy. After working as a postdoc at TU Braunschweig Germany, he joined Professor Marder's group at the Georgia Institute of Technology (2010-12 and 2018-19). He is currently an UGC-Assistant Professor under the University Grant Commission's faculty recharge program at Institute of Chemical Technology - Indian Oil Odisha Campus, Bhubaneswar).

Seth R. Marder obtained his B.A. from MIT Ph.D. from the University of Wisconsin and was a postdoc at the University of Oxford. In 2021, after positions at Caltech, JPL the University of Arizona, and Georgia Tech, he assumed the Directorship of the Renewable and Sustainable Energy Institute (RASEI), which is joint between the University of Colorado-Boulder (CUB) and the National Renewable Energy Laboratory (NREL). He is also a professor of Chemical and Biological Engineering and of Chemistry at CUB and a Senior Research Fellow at NREL He has received an NSF Special Creativity Award, the ACS Arthur C. Cope Scholar Award, Georgia Tech's Outstanding Faculty Research Author and Class of 1934 Distinguished Professor Awards, the MRS Mid-Career Award, and a Humboldt Research Award.

Stephen Barlow obtained his B.A. and D.Phil. in Chemistry from Oxford University in 1992 and 1996 respectively. After postdoctoral work at Caltech and a temporary faculty position at Oxford, he was a research scientist at the University of Arizona, and then at Georgia Tech. He has recently moved to CUB, where he is an Associate Research Professor in RASEI.

Author Contributions

The manuscript was written through contributions of all authors. All authors have given approval to the final version of the manuscript.

ACKNOWLEDGMENT

The authors are grateful to the coworkers and collaborators whose names appear in the cited references, and to funding agencies and companies that have supported our n-doping work: the National Science Foundation (through DMR-1305247, -1729737, and -1807797), Samsung Advanced Institute of Technology, Solvay, the Office of Naval Research (N00014-11-1-0313 and N00014-14-1-0171), and the Air Force Office of Scientific Research (FA9550B15B0115). SKM also thanks the University Grants Commission, Govt. of India for support through its faculty recharge program (F.4-5(155-FRP)/2014(BSR))"

REFERENCES

(1) Guo, S.; Kim, S. B.; Mohapatra, S. K.; Qi, Y.; Sajoto, T.; Kahn, A.; Marder, S. R.; Barlow, S. N-Doping of Organic Electronic Materials Using Air-Stable Organometallics. *Adv. Mater.* **2012**, *24*, 699-703.

(2) Mohapatra, S. K.; Fonari, A.; Risko, C.; Yesudas, K.; Moudgil, K.; Delcamp, J. H.; Timofeeva, T. V.; Brédas, J.-L.; Marder, S. R.; Barlow, S. Dimers of Nineteen-Electron Sandwich Compounds: Crystal and Electronic Structures, and Comparison of Reducing Strengths. *Chem. Eur. J.* **2014**, *20*, 15385-15394.

(3) Zhang, S.; Naab, B. D.; Jucov, E. V.; Parkin, S.; Evans, E. G. B.; Millhauser, G. L.; Timofeeva, T. V.; Risko, C.; Brédas, J.-L.; Bao, Z.; Barlow, S.; Marder, S. R. n-Dopants Based on Dimers of Benzimidazoline Radicals: Structures and Mechanism of Redox Reactions *Chem. Eur. J.* **2015**, *21*, 10878-10885.

(4) Lin, X.; Wegner, B.; Lee, K. M.; Fusella, M. A.; Zhang, F.; Moudgil, K.; Rand, B. P.; Barlow, S.; Marder, S. R.; Koch, N.; Kahn, A. Beating the Thermodynamic Limit with Photo-Activation of n-Doping in Organic Semiconductors. *Nat. Mater.* **2017**, *16*, 1209-1215.

(5) Walzer, K.; Maenning, B.; Pfeiffer, M.; Leo, K. Highly Efficient Organic Devices Based on Electrically Doped Transport Materials. *Chem. Rev.* **2007**, *107*, 1233-1271.

(6) Lüssem, B.; Keum, C.-M.; Kasemann, D.; Naab, B.; Bao, Z.; Leo, K. Doped Organic Transistors. *Chem. Rev.* **2016**, *116*, 13714-13751.

(7) Zhao, W.; Ding, J.; Zou, Y.; Di, C.-a.; Zhu, D. Chemical Doping of Organic Semiconductors for Thermoelectric Applications. *Chem. Soc. Rev.* **2020**, *49*, 7210-7228.

(8) Barlow, S.; Marder, S. R.; Lin, X.; Zhang, F.; Kahn, A. In *Handbook of Conducting Polymers, Fourth Edition*; Skotheim, T. A., Reynolds, J., Thompson, B. C., Eds.; CRC Press: 2019.
(9) Parthasarathy, G.; Shen, C.; Kahn, A.; Forrest, S. R. Lithium Doping of Semiconducting Organic Charge Transport Materials. *J. Appl. Phys.* **2001**, *89*, 4986-4992.
(10) Werner, A. G.; Li, F.; Harada, K.; Pfeiffer, M.; Fritz, T.; Leo, K. Pyronin B as a Donor for n-Type Doping of Organic Thin Films. *Appl. Phys. Lett.* **2003**, *82*, 4495-4497.
(11) Li, F.; Werner, A.; Pfeiffer, M.; Leo, K.; Liu, X. Leuco Crystal Violet as a Dopant for n-Doping of Organic Thin Films of Fullerene C_{60}. *J. Phys. Chem. B* **2004**, *108*, 17076-17082.
(12) Chan, C. K.; Kim, E.-G.; Brédas, J.-L.; Kahn, A. Molecular n-Type Doping of 1,4,5,8-Naphthalene Tetracarboxylic Dianhydride by Pyronin B Studied Using Direct and Inverse Photoelectron Spectroscopies. *Adv. Funct. Mater.* **2006**, *16*, 831-837.
(13) Wei, P.; Menke, T.; Naab, B. D.; Leo, K.; Riede, M.; Bao, Z. 2-(2-Methoxyphenyl)-1,3-dimethyl-1*H*-benzoimidazol-3-ium Iodide as a New Air-Stable n-Type Dopant for Vacuum-Processed Organic Semiconductor Thin Films. *J. Am. Chem. Soc.* **2012**, *134*, 3999–4002.
(14) Russ, B.; Robb, M. J.; Popere, B. C.; Perry, E. E.; Mai, C.-K.; Fronk, S. L.; Patel, S. N.; Mates, T. E.; Bazan, G. C.; Urban, J. J.; Chabinyc, M. L.; Hawker, C. J.; Segalman, R. A. Tethered Tertiary Amines as Solid-State n-Type Dopants for Solution-Processable Organic Semiconductors. *Chem. Sci.* **2016**, *7*, 1914-1919.
(15) Chueh, C.-C.; Li, C.-Z.; Ding, F.; Li, Z.; Cernetic, N.; Li, X.; Jen, A. K.-Y. Doping Versatile n-Type Organic Semiconductors via Room Temperature Solution-Processable Anionic Dopants. *ACS Appl. Mater. Interf.* **2017**, *9*, 1136-1144.
(16) Weber, C. D.; Bradley, C.; Lonergan, M. C. Solution Phase N-Doping of C_{60} and PCBM Using Tetrabutylammonium Fluoride. *J. Mater. Chem. A* **2014**, *2*, 303.
(17) Matsunaga, Y.; Goto, K.; Kubono, K.; Sako, K.; Shinmyozu, T. Photoinduced Color Change and Photomechanical Effect of Naphthalene Diimides Bearing Alkylamine Moieties in the Solid State. *Chem. Eur. J.* **2014**, *20*, 7309-7316.
(18) Wei, P.; Oh, J. H.; Dong, G.; Bao, Z. Use of a 1*H*-Benzoimidazole Derivative as an n-Type Dopant and to Enable Air-Stable Solution-Processed n-Channel Organic Thin-Film Transistors. *J. Am. Chem. Soc.* **2010**, *132*, 8852-8853.
(19) Naab, B. D.; Himmelberger, S.; Diao, Y.; Vandewal, K.; Wei, P.; Lussem, B.; Salleo, A.; Bao, Z. High Mobility n-Type Transistors Based on Solution-Sheared Doped 6,13-Bis(triisopropylsilylethynyl)pentacene Thin Films. *Adv. Mater.* **2013**, *25*, 4663-4667.
(20) Jhulki, S.; Un, H.-I.; Ding, Y.-F.; Risko, C.; Mohapatra, S. K.; Pei, J.; Barlow, S.; Marder, S. R. Reactivity of an Air-Stable Dihydrobenzoimidazole n-Dopant with Organic Semiconductor Molecules *Chem* **2021**, *7*, 1050-1065.
(21) Ziegler, K.; Ewald, L. Zur Kenntnis Des „Dreiwertigen" Kohlenstoffs. VII. Die Exakte Messung von Dissoziationsgleichgewichten. Bestimmung Der Dissoziationswärme Des Hexaphenyl-Äthans. *Annalen* **1929**, *473*, 163-193.
(22) Connelly, N. G.; Geiger, W. E. Chemical Redox Agents for Organometallic Chemistry. *Chem. Rev.* **1996**, *96*, 877-910.
(23) Schmakel, C. O.; Santhanam, K. S. V.; Elving, P. J. Nicotinamide Adenine Dinucleotide (NAD^+) and Related Compounds. Electrochemical Redox Pattern and Allied Chemical Behavior. *J. Am. Chem. Soc.* **1975**, *97*, 5083–5092.
(24) Kirkor, E. S.; Scheeline, A. Nicotinamide Adenine Dinucleotide Species in the Horseradish Peroxidase–Oxidase Oscillator. *Eur. J. Biochem.* **2000**, *267*, 5014-5022.

(25) Fukuzumi, S.; Suenobu, T.; Patz, M.; Hirasaka, T.; Itoh, S.; Fujitsuka, M.; Ito, O. Selective One-Electron and Two-Electron Reduction of C_{60} with NADH and NAD Dimer Analogues via Photoinduced Electron Transfer. *J. Am. Chem. Soc.* **1998**, *120*, 8060-8068.
(26) Ludvík, J.; Pragst, F.; Volke, J. Electrochemical Generation of Triplet States. Simplified Estimation of Triplet Energies by Electrogenerated Chemiluminescence Based on the Anodic Cleavage of Dimeric Dihydroheteroarenes. *J. Electroanal. Chem. Interfacial Electrochem.* **1984**, *180*, 141-156.
(27) Chan, C. K.; Amy, F.; Zhang, Q.; Barlow, S.; Marder, S. R.; Kahn, A. n-Type Doping of an Electron-Transport Material by Controlled Gas-Phase Doping with Cobaltocene. *Chem. Phys. Lett.* **2006**, *431*, 67-71.
(28) Chan, C. K.; Kahn, A.; Zhang, Q.; Barlow, S.; Marder, S. R. Incorporation of Cobaltocene as an *N*-Dopant in Organic Molecular Films. *J. Appl. Phys.* **2007**, *102*, 014906.
(29) Chan, C. K.; Zhao, W.; Barlow, S.; Marder, S. R.; Kahn, A. Decamethylcobaltocene as an Efficient n-Dopant in Organic Electronic Materials and Devices. *Org. Electron.* **2008**, *9*, 575-581.
(30) Collins, J. E.; Castellani, M. P.; Rheingold, A. L.; Miller, E. J.; Geiger, W. E.; Rieger, A. L.; Rieger, P. H. Synthesis, Characterization, and Molecular Structure of Bis(tetraphenylcyclopentdienyl)rhodium(II). *Organometallics* **1995**, *14*, 1232-1238.
(31) Lungwitz, D.; Schultz, T.; Tait, C. E.; Behrends, J.; Mohapatra, S. K.; Barlow, S.; Marder, S. R.; Opitz, A.; Koch, N. Disentangling Bulk and Interface Phenomena in a Molecularly Doped Polymer Semiconductor *Adv. Opt. Mater.* **2021**, *9*, 2002039.
(32) Fischer, E. O.; Wawersik, H. Über Aromatenkomplexe Von Metallen. LXXXVIII. Über Monomeres und Dimeres Dicyclopentadienylrhodium und Dicyclopentadienyliridium and über ein Neues Verfahren Zur Darstellung Ungeladener Metall-Aromaten-Komplexe. *J. Organomet. Chem.* **1966**, *5*, 559-567.
(33) El Murr, N.; Sheats, J. E.; Geiger, W. E.; Holloway, J. D. L. Electrochemical Reduction Pathways of the Rhodocenium Ion. Dimerization and Reduction of Rhodocene. *Inorg. Chem.* **1979**, *18*, 1443-1446.
(34) Gusev, O. V.; Denisovich, L. I.; Peterleitner, M. G.; Rubezhov, A. Z.; Ustynyuk, N. A.; Maitlis, P. M. Electrochemical Generation of 19- and 20-Electron Rhodocenium Complexes and Their Properties. *J. Organomet. Chem.* **1993**, *452*, 219-222.
(35) Gusev, O. V.; Peterleitner, M. G.; Ievlev, M. A.; Kal'sin, A. M.; Petrovskii, P. V.; Denisovich, L. I.; Ustynyuk, N. A. Reduction of Iridocenium Salts $[Ir(\eta^5\text{-}C_5Me_5)(\eta^5\text{-}L)]^+$ (L = C_5H_5, C_5Me_5, C_9H_7); Ligand-to-Ligand Dimerisation Induced by Electron Transfer. *J. Organomet. Chem.* **1997**, *531*, 95-100.
(36) Gusev, O. V.; Ievlev, M. A.; Peterleitner, M. G.; Peregudova, S. M.; Denisovich, L. I.; Petrovskii, P. V.; Ustynyuk, N. A. Reactions of Ruthenium Arenecyclopentadienyl Complexes. Reactions Induced by Electron Transfer. *J. Organomet. Chem.* **1997**, *534*, 57-66.
(37) Gusev, O. V.; Ievlev, M. A.; Peganova, T. A.; Peterleitner, M. G.; Petrovskii, P. V.; Oprunenko, Y. F.; Ustynyuk, N. A. Synthesis and Reduction of Trifluoromethyl-Substituted Arenecyclopentadienylruthenium Sandwiches $[Ru(\eta^5\text{-}C_5Me_4CF_3)(\eta^6\text{-}C_6R_6)]^+$ (R = H, Me) and $[Ru(\eta^5\text{-}C_5Me_5)(\eta^6\text{-}C_6H_5CF_3)]^+$ *J. Organomet. Chem.* **1998**, *551*, 93–100.
(38) Fischer, E. O.; Schmidt, M. W. Über Aromatenkomplexe Von Metallen, Cx. Über Fünfring- und Sechsring-Aromaten-π-Komplexe Des ^{99}Technetiums. *Chem. Ber.* **1969**, *102*, 1954-1960.

(39) Fischer, E. O.; Schmidt, M. W. Über Aromatenkomplexe Von Metallen, Xci. Über Monomeres und Dimeres Bis-Hexamethylbenzol-Rhenium. *Chem. Ber.* **1966**, *99*, 2206-2212.
(40) Nesmeyanov, A. N.; Vol'kenau, N. A.; Petrakova, V. A. Interaction of Electroneutral Benzenecyclopentadienyliron with Halogen Derivatives. *J. Organomet. Chem.* **1977**, *136*, 363-370.
(41) Hamon, J.-R.; Astruc, D.; Michaud, P. Syntheses, Characterizations, and Stereoelectronic Stabilization of Organometallic Electron Reservoirs: The 19-Electron d^7 Redox Catalysts η^5-$C_5R_5Fe^I$-η^6-$C_6R'_6$. *J. Am. Chem. Soc.* **1981**, *103*, 758-766.
(42) Rabâa, H.; Lacoste, M.; Delville-Desbois, M. H.; Ruiz, J.; Gloaguen, B.; Ardin, N.; Astruc, D.; Lebeuze, A.; Saillard, S. Y.; Linarès, J.; Varret, F.; Dance, S. M.; Marquestaut, E. Electronic Interplay between Two Iron Centers across Polyaromatic Ligands: Syntheses, Redox Chemistry, and Electronic Structures of the Electron-Reservoir 36- to 38-Electron Complexes $[(FeCp^*)\mu^2$-η^{12}-polyaromatic$)]^{q+}$ (q = 0-2) Including Mixed Valences and Biradicals. *Organometallics* **1995**, *14*, 5078-5092.
(43) Guo, S.; Mohapatra, S. K.; Romanov, A.; Timofeeva, T. V.; Hardcastle, K. I.; Yesudas, K.; Risko, C.; Brédas, J.-L.; Marder, S. R.; Barlow, S. N-Doping of Organic Electronic Materials Using Air-Stable Organometallics: A Mechanistic Study of Reduction by Dimeric Sandwich Compounds. *Chem. Eur. J.* **2012**, *18*, 14760-14772.
(44) Mohapatra, S. K.; Romanov, A.; Timofeeva, T. V.; Marder, S. R.; Barlow, S. Synthesis, Crystal Structures, and Redox Behavior of Some Pentamethylcyclopentadienyl Arene Ruthenium Salts. *J. Organomet. Chem.* **2014**, *751*, 314-320.
(45) Dye, J. L.; Cram, K. D.; Urbin, S. A.; Redko, M. Y.; Jackson, J. E.; Lefenfeld, M. Alkali Metals Plus Silica Gel: Powerful Reducing Agents and Convenient Hydrogen Sources. *J. Am. Chem. Soc.* **2005**, *127*, 9338-9339.
(46) Un, H.-I.; Gregory, S. A.; Mohapatra, S. K.; Xiong, M.; Longhi, E.; Lu, Y.; Rigin, S.; Jhulki, S.; Yang, C.-Y.; Timofeeva, T. V.; Wang, J.-Y.; Yee, S. K.; Barlow, S.; Marder, S. R.; Pei, J. Understanding the Effects of Molecular Dopant on N-Type Organic Thermoelectric Properties. *Adv. Energy Mater.* **2019**, *9*, 1900817.
(47) Longhi, E.; Risko, C.; Bacsa, J.; Khrustalev, V.; Rigin, S.; Moudgil, K.; Timofeeva, T. V.; Marder, S. R.; Barlow, S. Synthesis, Structures, and Reactivity of Isomers of $[RuCp^*(1,4$-$(Me_2N)_2C_6H_4)]_2$. *Dalton Trans.* **2021**, *50*, 13020-13030.
(48) Mohapatra, S. K.; Romanov, A.; Angles, G.; Timofeeva, T. V.; Barlow, S.; Marder, S. R. Synthesis and Characterization of Nonamethyl-Rhodocenium and Iridocenium Hexafluorophosphate Salts. *J. Organomet. Chem.* **2012**, *706-707*, 140-143.
(49) Lei, T.; Xia, X.; Wang, J.-Y.; Liu, C.-J.; Pei, J. "Conformation Locked" Strong Electron-Deficient Poly(P-Phenylene Vinylene) Derivatives for Ambient-Stable n-Type Field-Effect Transistors: Synthesis, Properties, and Effects of Fluorine Substitution Position. *J. Am. Chem. Soc.* **2014**, *136*, 2135-2141.
(50) Naab, B. D.; Zhang, S.; Vandewal, K.; Salleo, A.; Barlow, S.; Marder, S.; Bao, Z. Effective Solution- and Vacuum-Processed n-Doping by Dimers of Benzimidazoline Radicals. *Adv. Mater.* **2014**, *26*, 4268–4272.
(51) Yuan, D.; Huang, D.; Zhang, C.; Zou, Y.; Di, C.-a.; Zhu, X.; Zhu, D. Efficient Solution-Processed N-Type Small-Molecule Thermoelectric Materials Achieved by Precisely Regulating Energy Level of Organic Dopants. *ACS Appl. Mater. Interf.* **2017**, *9*, 28795-28801.

(52) Mohapatra, S. K.; Bacsa, J.; Jhulki, S.; Conte, M.; Kurdi, K. A.; Barlow, S.; Marder, S. R. *unpublished*.
(53) Moudgil, K.; Mann, M. A.; Risko, C.; Bottomley, L. A.; Marder, S. R.; Barlow, S. Dimers of Nineteen-Electron Sandwich Compounds: An Electrochemical Study of the Kinetics of Their Formation. *Organometallics* **2015**, *34*, 3706–3712.
(54) Zavitsas, A. A. The Relation between Bond Lengths and Dissociation Energies of Carbon-Carbon Bonds. *J. Phys. Chem. A* **2003**, *107*, 897-898.
(55) Perry, E.; Chiu, C.-Y.; Moudgil, K.; Schlitz, R.; Takacs, C.; O'Hara, K.; Labram, J.; Glaudell, A.; Sherman, J.; Barlow, S.; Hawker, C. J.; Marder, S. R.; Chabinyc, M. L. High Conductivity in a Non-Planar n-Doped Ambipolar Semiconducting Polymer. *Chem. Mater.* **2017**, *29*, 9742-9750.
(56) Yamashita, Y.; Jhulki, S.; Bhardwaj, D.; Longhi, E.; Kumagai, S.; Watanabe, S.; Barlow, S.; Marder, S. R.; Takeya, J. Highly Air-Stable, n-Doped Conjugated Polymers Achieved by Dimeric Organometallic Dopants. *J. Mater. Chem. C* **2021**, *9*, 4105-4110.
(57) Olthof, S.; Mohapatra, S. K.; Barlow, S.; Mehraeen, S.; Coropceanu, V.; Brédas, J.-L.; Marder, S. R.; Kahn, A. Ultralow Doping in Organic Semiconductors: Evidence of Trap Filling. *Phys. Rev. Lett.* **2012**, *109*, 176601.
(58) Higgins, A.; Mohapatra, S. K.; Barlow, S.; Marder, S. R.; Kahn, A. Dopant Controlled Trap-Filling and Conductivity Enhancement in an Electron-Transport Polymer. *Appl. Phys. Lett.* **2015**, *106*, 163301.
(59) Zhang, Y.; Phan, H.; Zhou, H.; Zhang, X.; Zhou, J.; Moudgil, K.; Barlow, S.; Marder, S. R.; Facchetti, A.; Nguyen, T.-Q. Electron Transport and Nanomorphology in Solution-Processed Polymeric Semiconductor n-Doped with an Air-Stable Organometallic Dimer. *Adv. Electron. Mater.* **2017**, *3*, 1600546.
(60) Smith, H. L.; Dull, J. T.; Barlow, S.; Rand, B. P.; Marder, S. R.; Kahn, A. n-Doping of Low-Electron-Affinity Polymer Used as an Electron-Transport Layer in Organic Light-Emitting Diodes. *Adv. Funct. Mater.* **2020**, *30*, 2000328.
(61) Guan, Z.-L.; Kim, J. B.; Wang, H.; Jaye, C.; Fischer, D. A.; Loo, Y.-L.; Kahn, A. Direct Determination of the Electronic Structure of the Poly(3-Hexylthiophene):Phenyl-[6,6]-C_{61} Butyric Acid Methyl Ester Blend. *Org. Electron.* **2010**, *11*, 1779-1785.
(62) Li, J.; Rochester, C. W.; Jacobs, I. E.; Aasen, E. W.; Friedrich, S.; Stroeve, P.; Moulé, A. J. The Effect of Thermal Annealing on Dopant Site Choice in Conjugated Polymers. *Org. Electron.* **2016**, *33*, 23-31.
(63) Olthof, S.; Singh, S.; Mohapatra, S. K.; Barlow, S.; Marder, S. R.; Kippelen, B.; Kahn, A. Passivation of Trap States in Unpurified and Purified C_{60} and the Influence on Organic Field-Effect Transistor Performance. *Appl. Phys. Lett.* **2012**, *101*, 253303.
(64) Singh, S.; Mohapatra, S. K.; Sharma, A.; Fuentes-Hernandez, C.; Barlow, S.; Marder, S. R.; Kippelen, B. Reduction of Contact Resistance by Selective Contact Doping in Fullerene N-Channel Organic Field-Effect Transistors. *Appl. Phys. Lett.* **2013**, *102*, 153303.
(65) Paniagua, S. A.; Baltazar, J.; Sojoudi, H.; Mohapatra, S. K.; Zhang, S.; Henderson, C. L.; Graham, S.; Barlow, S.; Marder, S. R. Production of Heavily n- and p-Doped CVD Graphene with Solution-Processed Redox-Active Metal-Organic Species. *Mater. Horiz.* **2014**, *1*, 111-115.
(66) Zhang, F.; Klein, C.; Longhi, E.; Barlow, S.; Marder, S. R.; Sarusi, G.; Kahn, A. Molecular-Reductant-Induced Control of a Graphene–Organic Interface for Electron Injection. *Chem. Mater.* **2019**, *31*, 6624-6632.

(67) Guo, R.; Zheng, Y.; Hu, Z.; Zhang, J.; Han, C.; Longhi, E.; Barlow, S.; Marder, S. R.; Chen, W. Surface Functionalization of Black Phosphorus with a Highly Reducing Organoruthenium Complex: Interface Properties and Enhanced Photoresponsivity of Photodetectors. *Chem. Eur. J.* **2020**, *26*, 6576-6582.
(68) Tarasov, A.; Zhang, S.; Tsai, M.-Y.; Campbell, P. M.; Graham, S.; Barlow, S.; Marder, S. R.; Vogel, E. M. Controlled Doping of Large-Area Trilayer MoS_2 with Molecular Reductants and Oxidants. *Adv. Mater.* **2015**, *27*, 1175-1181.
(69) Guo, R.; Li, Q.; Zheng, Y.; Lei, B.; Sun, H.; Hu, Z.; Zhang, J.; Wang, L.; Longhi, E.; Barlow, S.; Marder, S. R.; Wang, J.; Chen, W. Degenerate Electron-Doping in Two-Dimensional Tungsten Diselenide with a Dimeric Organometallic Reductant. *Mater. Today* **2019**, *30*, 26-33.
(70) Schlesinger, R.; Blumstengel, S.; Christodoulou, C.; Ovsyannikov, R.; Kobin, B.; Moudgil, K.; Barlow, S.; Hecht, S.; Marder, S. R.; Henneberger, F.; Koch, N. Efficient Light Emission from Inorganic and Organic Semiconductor Hybrid Structures by Energy-Level Tuning. *Nat. Commun.* **2015**, *6*, 6754.
(71) Giordano, A. J.; Pulvirenti, F.; Khan, T. M.; Fuentes-Hernandez, C.; Moudgil, K.; Delcamp, J. H.; Kippelen, B.; Barlow, S.; Marder, S. R. Organometallic Dimers: Application to Work-Function Reduction of Conducting Oxides *ACS Appl. Mater. Interf.* **2015**, *7*, 4320-4326.
(72) Schultz, T.; Lungwitz, D.; Longhi, E.; Barlow, S.; Marder, S. R.; Koch, N. The Interlayer Method: A Universal Tool for Energy Level Alignment Tuning at Inorganic/Organic Semiconductor Heterojunctions. *Adv Funct. Mater.* **2021**, *31*, 2010174.
(73) Zhao, L.; Roh, K.; Kacmoli, S.; Kurdi, K. A.; Jhulki, S.; Barlow, S.; Marder, S. R.; Gmachl, C.; Rand, B. P. Thermal Management Enables Bright and Stable Perovskite Light-Emitting Diodes. *Adv. Mater.* **2020**, *32*, 2000752.
(74) Pulvirenti, F.; Wegner, B.; Noel, N. K.; Mazzotta, G.; Hill, R.; Patel, J. B.; Herz, L. M.; Johnston, M. B.; Riede, M. K.; Snaith, H. J.; Koch, N.; Barlow, S.; Marder, S. R. Modification of the Fluorinated Tin Oxide/Electron-Transporting Material Interface by a Strong Reductant and Its Effect on Perovskite Solar Cell Efficiency. *Mol. Syst. Des. Eng.* **2018**, *3*, 741-747.
(75) Reiser, P.; Benneckendorf, F. S.; Barf, M.-M.; Müller, L.; Bäuerle, R.; Hillebrandt, S.; Beck, S.; Lovrincic, R.; Mankel, E.; Freudenberg, J.; Jänsch, D.; Kowalsky, W.; Pucci, A.; Jaegermann, W.; Bunz, U. H. F.; Müllen, K. n-Type Doping of Organic Semiconductors: Immobilization via Covalent Anchoring. *Chem. Mater.* **2019**, *31*, 4213-4221.